

---

# Time Series Deconfounder: Estimating Treatment Effects over Time in the Presence of Hidden Confounders

---

Ioana Bica<sup>1 2</sup> Ahmed M. Alaa<sup>3</sup> Mihaela van der Schaar<sup>2 3 4</sup>

## Abstract

The estimation of treatment effects is a pervasive problem in medicine. Existing methods for estimating treatment effects from longitudinal observational data assume that there are no hidden confounders. This assumption is not testable in practice and, if it does not hold, leads to biased estimates. In this paper, we develop the Time Series Deconfounder, a method that leverages the assignment of multiple treatments over time to enable the estimation of treatment effects in the presence of multi-cause hidden confounders. The Time Series Deconfounder uses a novel recurrent neural network architecture with multitask output to build a factor model over time and infer substitute confounders that render the assigned treatments conditionally independent. Then it performs causal inference using the substitute confounders. We provide a theoretical analysis for obtaining unbiased causal effects of time-varying exposures using the Time Series Deconfounder. Using both simulations and real data to show the effectiveness of our method in deconfounding the estimation of treatment responses in longitudinal data.

## 1. Introduction

Forecasting the patient’s response to treatments assigned over time represents a crucial problem in the medical domain. The increasing availability of observational data makes it possible to learn individualized treatment responses from longitudinal disease trajectories containing information about patient covariates and treatment assignments (Robins et al., 2000a; Robins & Hernán, 2008; Schulam & Saria, 2017; Lim et al., 2018; Bica et al., 2020). However, existing methods assume that all confounders — variables

affecting the treatment assignments and the potential outcomes — are observed, an assumption which is not testable in practice<sup>1</sup> and probably not true in many situations.

To understand why the presence of hidden confounders introduces bias, consider the problem of estimating treatment effects for patients with cancer. They are often prescribed multiple treatments at the same time, including chemotherapy, radiotherapy and/or immunotherapy based on their tumour characteristics. These treatments are adjusted if the tumour size changes. The treatment strategy is also changed as the patient starts to develop drug resistance (Vlachostergios & Faltas, 2018) or the toxicity levels of the drugs increase (Kroschinsky et al., 2017). Drug resistance and toxicity levels are multi-cause confounders since they affect not only the multiple causes (treatments), but also the patient outcome (e.g. mortality, risk factors). However, drug resistance and toxicity may not be observed and, even if observed, may not be recorded in the electronic health records. Estimating, for instance, the effect of chemotherapy on the cancer progression in the patient without accounting for the dependence on drug resistance and toxicity levels (hidden confounders) will produce biased results.

Wang & Blei (2019a) developed theory for deconfounding — adjusting for the bias introduced by the existence of hidden confounders in observational data — in the *static* causal inference setting and noted that the existence of multiple causes makes this task easier. Wang & Blei (2019a) observed that the dependencies in the assignment of multiple causes in the static setting can be used to infer latent variables that render the causes independent and act as substitutes for the hidden confounders.

In this paper, we propose the Time Series Deconfounder, a method that enables the unbiased estimation of treatment responses *over time* in the presence of hidden confounders, by taking advantage of the sequential assignment of multiple treatments. We draw from the main idea in Wang & Blei (2019a), but note that the estimation of hidden confounders in the longitudinal setting is significantly more complex than in the static setting, not just because the hidden confounders may vary over time but in particular because the hidden

---

<sup>1</sup>University of Oxford, Oxford, United Kingdom <sup>2</sup>The Alan Turing Institute, London, United Kingdom <sup>3</sup>UCLA, Los Angeles, USA <sup>4</sup>University of Cambridge, Cambridge, United Kingdom. Correspondence to: Ioana Bica <ioana.bica@eng.ox.ac.uk>.

---

<sup>1</sup>Since counterfactuals are never observed, it is not possible to test for the existence of hidden confounders that could affect them.

confounders may be affected by previous treatments and covariates. In this case, standard latent variable models are no longer applicable, as they cannot capture these time dependencies.

The Time Series Deconfounder relies on building a factor model *over time* to obtain substitutes for the hidden confounder which, together with the observed variables render the assigned causes conditionally independent. Through theoretical analysis we show how the substitute confounders can be used to satisfy the strong ignorability condition in the potential outcomes framework for time-varying exposures (Robins & Hernán, 2008) and obtain unbiased estimates of individualized treatment responses, using weaker assumptions than standard methods. Following our theory, we propose a novel deep learning architecture, based on a recurrent neural network with multi-task output and variational dropout to build such a factor model and infer substitutes for the hidden confounders in practice.

The Time Series Deconfounder shifts the need for observing all confounders (untestable condition) to constructing a good factor model over time (testable condition). To assess how well the factor model captures the distribution of assigned causes, we extend the use of predictive checks (Rubin, 1984; Wang & Blei, 2019a) over time and compute  $p$ -values at each timestep. We perform experiments on a simulated dataset where we control the amount of hidden confounding applied and a real dataset with patients in the ICU (Johnson et al., 2016) to show how the Time Series Deconfounder allows us to deconfound the estimation of treatment responses in longitudinal data. To the best of our knowledge, this represents the first method for learning hidden confounders in the time series setting.

## 2. Related Work

Previous methods for causal inference mostly focused on the static setting (Hill, 2011; Wager & Athey, 2017; Alaa & van der Schaar, 2017; Yoon et al., 2018; Alaa & Schaar, 2018), and less attention has been given to the time series setting. We discuss methods for estimating treatment effects over time, as well as methods for inferring substitute hidden confounders in the static setting.

**Potential outcomes for time-varying treatment assignments.** Standard methods for performing counterfactual inference in longitudinal data are found in the epidemiology literature and include the  $g$ -computation formula,  $g$ -estimation of structural nested mean models and inverse probability of weighting estimation of marginal structural models (Robins, 1986; 1994; Robins et al., 2000a; Robins & Hernán, 2008). Additionally, (Lim et al., 2018) improves on the standard marginal structural models by using recurrent neural networks to estimate the propensity weights and

treatment response. While these methods have been widely used in forecasting treatment responses, they are all based on the assumption that there are no hidden confounders in the observational data. Our paper proposes a method for deconfounding such outcome models, by inferring substitutes for the hidden confounders which can lead to unbiased estimates of the potential outcomes.

The potential outcomes framework has been extended to the continuous time setting by (Lok et al., 2008). Several methods have been proposed for estimating the treatment responses in continuous time (Xu et al., 2016; Soleimani et al., 2017; Schulam & Saria, 2017), again assuming that there are no hidden confounders. Here, we focus on deconfounding the estimation of treatment responses in the discrete time setting.

Sensitivity analysis methods which evaluate the potential impact that an unmeasured confounder could have on the estimation of treatment effect have also been developed (Robins et al., 2000b; Roy et al., 2016; Scharfstein et al., 2018). However, these methods assess the suitability of applying existing tools, rather than propose a direct solution for handling unobserved hidden confounders.

**Latent variable models for estimating hidden confounders.** The most similar work to ours is the one of Wang & Blei (2019a), who proposed the deconfounder, an algorithm that infers latent variables that act as substitutes for the hidden confounders and then performs causal inference in the static multi-cause setting. The deconfounder involves finding a good factor model of the assigned causes which can be used to estimate the substitute confounders. Then, the deconfounder fits an outcome model for estimating the causal effects using the inferred latent variables. Our paper extends the theory for the deconfounder to the time-varying treatments setting and shows how the inferred latent variables can lead to sequential strong ignorability. To estimate the substitute confounders, Wang & Blei (2019a) used standard factor models (Tipping & Bishop, 1999; Ranganath et al., 2015), which are only applicable in the static setting. To build a factor model over time, we propose an RNN architecture with multitask output and variational dropout.

Several methods have been proposed for taking advantage of the multiplicity of assigned causes in the static setting and capture shared latent confounding (Tran & Blei, 2017; Heckerman, 2018; Ranganath & Perotte, 2018). However, these works are based on Pearl’s causal framework (Pearl, 2009) and use structural equation models, while our method deconfounds the estimation of treatment effects in the potential outcomes framework (Neyman, 1923; Rubin, 1978; Robins & Hernán, 2008). Alternative methods for dealing with hidden confounders in the static setting involve using proxy variables as noisy substitutes for latent confounders (Lash et al., 2014; Louizos et al., 2017; Lee et al., 2018).

### 3. Problem Formulation

Let the random variables  $\mathbf{X}_t^{(i)} \in \mathcal{X}_t$  be the time-dependent covariates for patient  $(i)$  and  $\mathbf{A}_t^{(i)} = [A_{t1}^{(i)} \dots A_{tk}^{(i)}] \in \mathcal{A}_t$  be the possible assignment of  $k$  treatments (causes) at time  $t$ . Treatments can be either binary and/or continuous. Static features, such as genetic information, do not change our theory and, for simplicity, we assume they are part of the observed covariates. We want to estimate the effect of the treatments assigned until timestep  $T^{(i)}$  on an outcome of interest  $\mathbf{Y}^{(i)} \in \mathcal{Y}$ , observed at timestep  $T^{(i)} + 1$ .

Observational data about the patient consists of realizations of the previously described random variables:  $\mathcal{D}^{(i)} = \{\mathbf{x}_t^{(i)}, \mathbf{a}_t^{(i)}\}_{t=1}^{T^{(i)}} \cup \{\mathbf{y}_{T^{(i)}+1}^{(i)}\}$ , with samples collected at discrete and regular timesteps. Electronic health records consist of data for  $N$  independent patients. For simplicity, we omit the patient superscript  $(i)$  unless it is explicitly needed.

Let  $\bar{\mathbf{A}}_t = (\mathbf{A}_1, \dots, \mathbf{A}_t) \in \bar{\mathcal{A}}_t$  be the history of treatments and let  $\bar{\mathbf{X}}_t = (\mathbf{X}_1, \dots, \mathbf{X}_t) \in \bar{\mathcal{X}}_t$  be the history of covariates until timestep  $t$ . Let  $\bar{\mathbf{A}} = \bar{\mathbf{A}}_T$  and  $\bar{\mathbf{X}} = \bar{\mathbf{X}}_T$  be the entire treatment and covariate history respectively, with  $\bar{\mathbf{A}} \in \bar{\mathcal{A}} = \bar{\mathcal{A}}_T$  and  $\bar{\mathbf{X}} \in \bar{\mathcal{X}} = \bar{\mathcal{X}}_T$  and let  $\bar{\mathbf{a}} \in \bar{\mathcal{A}}$  and  $\bar{\mathbf{x}} \in \bar{\mathcal{X}}$  be realisations of these random variables.

We adopt the potential outcomes framework proposed by Rubin (1978) and Neyman (1923), and extended by Robins & Hernán (2008) to take into account time-varying treatments to estimate the effect of  $\bar{\mathbf{A}}$  on  $\mathbf{Y}$ . Let  $\mathbf{Y}(\bar{\mathbf{a}})$  be the potential outcome, either factual or counterfactual, for the treatment history  $\bar{\mathbf{a}}$ . For each patient, we aim to estimate individualized treatment responses, i.e. treatment outcomes conditional on patient covariates:  $\mathbb{E}[\mathbf{Y}(\bar{\mathbf{a}}) \mid \bar{\mathbf{X}}]$ . The observational data can be used to obtain  $\mathbb{E}[\mathbf{Y} \mid \bar{\mathbf{A}} = \bar{\mathbf{a}}, \bar{\mathbf{X}}]$ . Under certain assumptions, these estimates are unbiased so that  $\mathbb{E}[\mathbf{Y}(\bar{\mathbf{a}}) \mid \bar{\mathbf{X}}] = \mathbb{E}[\mathbf{Y} \mid \bar{\mathbf{A}} = \bar{\mathbf{a}}, \bar{\mathbf{X}}]$ . These conditions include Assumptions 1 and 2, which are standard among the existing methods and can be tested in practice (Robins & Hernán, 2008).

**Assumption 1: Consistency.** If  $\bar{\mathbf{A}} = \bar{\mathbf{a}}$  for a given patient, then  $\mathbf{Y}(\bar{\mathbf{a}}) = \mathbf{Y}$  for that patient.

**Assumption 2: Positivity (Overlap)** (Imai & Van Dyk, 2004): If  $P(\bar{\mathbf{A}}_{t-1} = \bar{\mathbf{a}}_{t-1}, \bar{\mathbf{X}}_t = \bar{\mathbf{x}}_t) \neq 0$  then  $P(\bar{\mathbf{A}}_t = \bar{\mathbf{a}}_t \mid \bar{\mathbf{A}}_{t-1} = \bar{\mathbf{a}}_{t-1}, \bar{\mathbf{X}}_t = \bar{\mathbf{x}}_t) > 0$  for all  $\bar{\mathbf{a}}_t$ .

In addition to these two assumptions, existing methods also assume *sequential strong ignorability*:

$$\mathbf{Y}(\bar{\mathbf{a}}) \perp\!\!\!\perp \mathbf{A}_t \mid \bar{\mathbf{A}}_{t-1}, \bar{\mathbf{X}}_t, \quad (1)$$

for all  $\bar{\mathbf{a}} \in \bar{\mathcal{A}}$  and for all  $t = 1, \dots, T$ . This condition holds if there are no hidden confounders, an assumption which is untestable in practice. To understand why this is the case, note that the sequential strong ignorability assumption requires the conditional independence of the treatments with

all of the potential outcomes, both factual and counterfactual. Since the counterfactuals are never observed, it is not possible to test for this conditional independence.

We assume that there are hidden confounders. Consequently, using standard methods for computing  $\mathbb{E}[\mathbf{Y} \mid \bar{\mathbf{A}}, \bar{\mathbf{X}}]$  from the dataset will result in biased estimates since the hidden confounders introduce a dependence between the treatments at each timestep and the potential outcomes ( $\mathbf{Y}(\bar{\mathbf{a}}) \not\perp\!\!\!\perp \mathbf{A}_t \mid \bar{\mathbf{A}}_{t-1}, \bar{\mathbf{X}}_t$ ) and therefore:

$$\mathbb{E}[\mathbf{Y}(\bar{\mathbf{a}}) \mid \bar{\mathbf{X}}] \neq \mathbb{E}[\mathbf{Y} \mid \bar{\mathbf{A}} = \bar{\mathbf{a}}, \bar{\mathbf{X}}]. \quad (2)$$

By extending the method proposed by (Wang & Blei, 2019a), we take advantage of the multiple treatment assignments at each timestep to infer a sequence of latent variables  $\bar{\mathbf{Z}} = (\mathbf{Z}_1, \dots, \mathbf{Z}_T) \in \bar{\mathcal{Z}}$  that can be used as substitutes for the unobserved confounders. We will then show how  $\bar{\mathbf{Z}}$  can be used to estimate the treatment effects.

### 4. Time Series Deconfounder

The idea behind the Time Series Deconfounder is that multi-cause confounders introduce dependencies between the treatments. As treatment assignments change over time we infer substitutes for the hidden confounders that take advantage of patient history to capture these dependencies.

#### 4.1. Factor Model

The Time Series Deconfounder builds a factor model to capture the distribution of the causes over time. At time  $t$ , the factor model constructs the latent variable  $\mathbf{z}_t = g(\bar{\mathbf{h}}_{t-1})$ , where  $\bar{\mathbf{h}}_{t-1} = (\bar{\mathbf{a}}_{t-1}, \bar{\mathbf{x}}_{t-1}, \bar{\mathbf{z}}_{t-1})$  is the realisation of history  $\bar{\mathbf{H}}_{t-1}$ . Together with the observed covariates,  $\mathbf{z}_t$  renders the assigned causes conditionally independent  $p(a_{t1}, \dots, a_{tk} \mid \mathbf{z}_t, \mathbf{x}_t) = \prod_{j=1}^k p(a_{tj} \mid \mathbf{z}_t, \mathbf{x}_t)$ . Figure 1(a) illustrates the corresponding graphical model for timestep  $t$ .

The factor model of the assigned causes is a latent variable model with joint distribution:

$$p(\theta_{1:k}, \bar{\mathbf{x}}, \bar{\mathbf{z}}, \bar{\mathbf{a}}) = p(\theta_{1:k})p(\bar{\mathbf{x}}) \cdot \prod_{t=1}^T (p(\mathbf{z}_t \mid \bar{\mathbf{h}}_{t-1}) \prod_{j=1}^k p(a_{tj} \mid \mathbf{z}_t, \mathbf{x}_t, \theta_j)), \quad (3)$$

where  $\theta_{1:k}$  are parameters. The distribution of assigned causes  $p(\bar{\mathbf{a}})$  is the corresponding marginal.

By taking advantage of the dependencies between the multiple treatment assignments, the factor model allows us to infer the sequence of latent variables  $\bar{\mathbf{Z}}$  that render the assigned causes conditionally independent. Through this factor model construction and under correct model specifica-

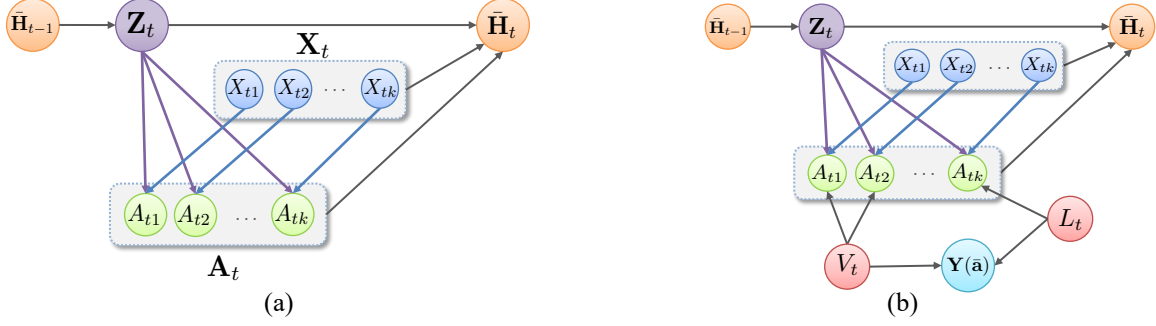


Figure 1. (a) Graphical factor model. Each  $Z_t$  is built as a function of the history, such that, with  $X_t$ , it renders the assigned causes conditionally independent:  $p(a_{t1}, \dots, a_{tk} | z_t, x_t) = \prod_{j=1}^k p(a_{tj} | z_t, x_t)$ . The variables can be connected to  $Y(\bar{a})$  in any way. (b) Graphical model explanation for why this factor model construction ensures that  $Z_t$  captures all of the multi-cause hidden confounders.

tions, we can rule out the existence of other multi-cause confounders which are not captured by  $Z_t$ . Consider the graphical model in Figure 1(b). By contradiction, assume that there exists another multi-cause confounder  $V_t$  not captured by  $Z_t$ . Then, by  $d$ -separation the conditional independence between the assigned causes given  $Z_t$  and  $X_t$  does not hold any more. This argument cannot be used for single-cause confounders, such as  $L_t$ , which are only affecting one of the causes and the potential outcomes. Thus, we assume sequential single strong ignorability (no hidden single cause confounders).

**Assumption 3: Sequential single strong ignorability:**

$$Y(\bar{a}) \perp\!\!\!\perp A_{tj} | X_t, \bar{H}_{t-1}, \quad (4)$$

$$\forall \bar{a} \in \bar{\mathcal{A}} \text{ and } \forall t \in \{0, \dots, T\} \text{ and } \forall j \in \{1, \dots, k\}.$$

Causal inference relies on assumptions. Existing methods for estimating treatment affects over time assume that there are no multi-cause and single-cause hidden confounders. In this paper, we make the *weaker* assumption that there are no single-cause hidden confounders. While this assumption is also untestable in practice, as the number of causes increases for each timestep, it becomes increasingly weaker: the more causes we observe, the less likely it becomes for a hidden confounder to affect only one of them.

**Theorem 1:** If the distribution of the assigned causes  $p(\bar{a})$  can be written as the factor model  $p(\theta_{1:k}, \bar{x}, \bar{z}, \bar{a})$ , we obtain *sequential ignorable treatment assignment*:

$$Y(\bar{a}) \perp\!\!\!\perp (A_{t1}, \dots, A_{tk}) | \bar{A}_{t-1}, \bar{X}_t, \bar{Z}_t, \quad (5)$$

for all  $\bar{a} \in \bar{\mathcal{A}}$  and for all  $t \in \{0, \dots, T\}$ . Theorem 1 is proved by leveraging Assumption 3, the fact that the substitute confounders  $Z_t$  are inferred without knowledge of the potential outcomes  $Y(\bar{a})$  and the fact that the causes  $(A_{t1}, \dots, A_{tk})$  are jointly independent given  $Z_t$  and  $X_t$ . The result means that, at each timestep, the variables  $\bar{X}_t, \bar{Z}_t, \bar{A}_{t-1}$  contain all of the dependencies between the potential outcomes and the assigned causes  $\bar{A}_t$ . See Appendix A for the full proof.

As discussed in Wang & Blei (2019a); DAmour (2019), to identify the causal effects, the substitute confounders  $Z_t$  also need to satisfy positivity (Assumption 2), i.e.  $P(\bar{A}_t = \bar{a}_t | \bar{A}_{t-1} = \bar{a}_{t-1}, \bar{Z}_t = \bar{z}_t, \bar{X}_t = \bar{x}_t) > 0$ . After fitting the factor model, this can be tested (Robins & Hernán, 2008). When positivity is limited, the outcome model estimates of treatment responses will also have high variance. In practice, positivity can be enforced by setting the dimensionality of  $Z_t$  to be smaller than the number of causes (Wang & Blei, 2019a).

**Predictive Checks over Time:** The theory holds if the fitted factor model captures well the distribution of assigned causes. This condition can be assessed by extending predictive model checking (Rubin, 1984) to the time-series setting. We compute  $p$ -values over time to evaluate how similar the distribution of the treatments learnt by the factor model is with the distribution of the treatments in a validation set of patients. At each timestep  $t$ , for the patients in the validation set, we obtain  $M$  replicas of their treatment assignments  $\{\mathbf{a}_{t, \text{rep}}^{(i)}\}_{i=1}^M$  by sampling from the factor model. The replicated treatment assignments are compared with the actual treatment assignments,  $\mathbf{a}_{t, \text{val}}$ , using the test statistic  $T(\mathbf{a}_t)$ :

$$T(\mathbf{a}_t) = \mathbb{E}_Z[\log p(\mathbf{a}_t | Z_t, X_t)], \quad (6)$$

related to the marginal log likelihood (Wang & Blei, 2019a). The predictive  $p$ -value for timestep  $t$  is computed as follows:

$$\frac{1}{M} \sum_{i=1}^M \mathbf{1} \left( T \left( \mathbf{a}_{t, \text{rep}}^{(i)} \right) < T \left( \mathbf{a}_{t, \text{val}} \right) \right), \quad (7)$$

where  $\mathbf{1}(\cdot)$  represents the indicator function.

If the model captures well the distribution of the assigned causes, then the test statistics for the treatment replicas are similar to the test statistic for the treatments in the validation set, which makes 0.5 the ideal  $p$ -value in this case.

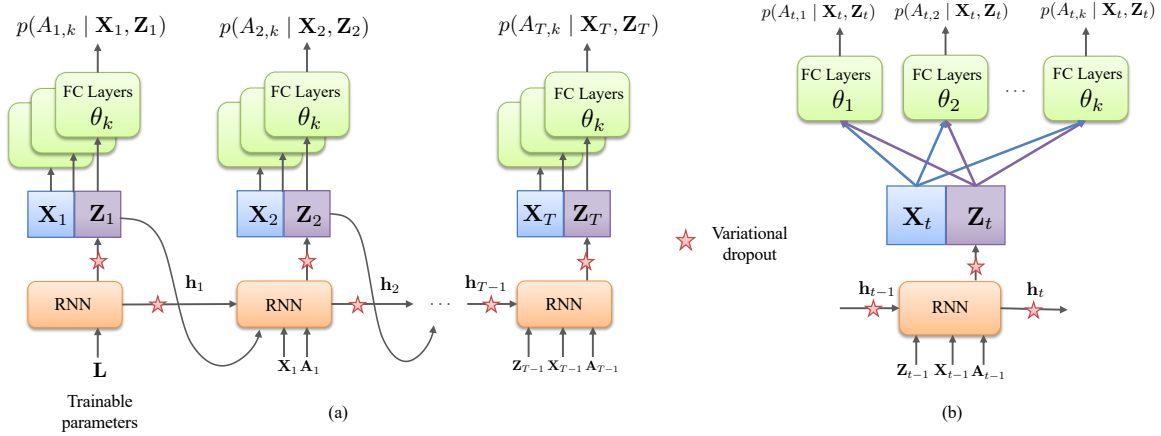


Figure 2. (a) Proposed factor model implementation.  $\mathbf{Z}_t$  is generated by RNN as a function of the history  $\bar{\mathbf{H}}_{t-1}$ , given by the hidden state  $\mathbf{h}_t$ , and current input. Multitask output is used to construct the treatments such that they are independent given  $\mathbf{Z}_t$  and  $\mathbf{X}_t$ . (b) Closer look at a single timestep.

## 4.2. Outcome Model

If the factor model passes the predictive checks, the Time Series Deconfounder fits an outcome model (Robins et al., 2000a; Lim et al., 2018) to estimate  $\mathbb{E}[\mathbf{Y} \mid \bar{\mathbf{A}} = \bar{\mathbf{a}}, \bar{\mathbf{X}}, \hat{\hat{\mathbf{Z}}}]$ , where  $\hat{\hat{\mathbf{Z}}}$  is sampled from the factor model. To compute **uncertainty estimates of the potential outcomes**, we can sample  $\hat{\hat{\mathbf{Z}}}$  repeatedly and then fit an outcome model for each sample to obtain multiple point estimates of  $\mathbf{Y}$ . The variance of these point estimates will represent the uncertainty of the Time Series Deconfounder.

DAmour (2019) raised some concerns about identifiability of the mean potential outcomes using the deconfounder framework in Wang & Blei (2019a) in the static setting and illustrated some pathological examples where identifiability might not hold.<sup>2</sup> In practical settings, the outcome estimates from the Time Series Deconfounder are identifiable, as supported by the experimental results in Sections 6 and 7. Nevertheless, when identifiability represents an issue, the uncertainty in the potential outcomes can be used to assess the reliability of the Time Series Deconfounder. In particular, the variance in the potential outcomes indicates how *the finite observational data* informs the estimation of substitutes for the hidden confounders and subsequently the treatment outcomes of interest. When the treatment effects are non-identifiable, the estimates of the Time Series Deconfounder will have high variance.

By using this framework to estimate substitutes for the hidden confounders we are trading off confounding bias for estimation variance (Wang & Blei, 2019a). The treatment effects computed without accounting for the hidden confounders will inevitably be biased. Alternatively, using the

<sup>2</sup>See Wang & Blei (2019a) for a longer discussion addressing the concerns in (DAmour, 2019).

substitute confounders from the factor model will result in unbiased, but higher variance estimates of treatment effects.

## 5. Factor Model over Time in Practice

Since we are dealing with time-varying treatments, we cannot use standard factor models, such as PCA (Tipping & Bishop, 1999) or Deep Exponential Families (Ranganath et al., 2015), as they can only be applied in the static setting. Using the theory developed for the factor model over time we introduce a practical implementation based on an RNN with multitask output and variational dropout as illustrated in Figure 2.

The recurrent part of the model infers the substitute confounders such that they depend on the history:  $\mathbf{Z}_1 = \text{RNN}(\mathbf{L})$  and  $\mathbf{Z}_t = \text{RNN}(\bar{\mathbf{Z}}_{t-1}, \bar{\mathbf{X}}_{t-1}, \bar{\mathbf{A}}_{t-1}, \mathbf{L})$ , where  $\mathbf{L}$  consists of randomly initialized parameters and trained with the rest of the parameters in the RNN. The size of the RNN output is  $D_Z$  and this specifies the size of the substitute confounders. In our experiments, we use the LSTM unit (Hochreiter & Schmidhuber, 1997). Moreover, to infer the assigned causes at timestep  $t$ ,  $\mathbf{A}_t = [A_{t1}, \dots, A_{tk}]$  such that they are conditionally independent given the latent variable  $\mathbf{Z}_t$  and the observed covariates  $\mathbf{X}_t$ , we propose using multitask multilayer perceptrons (MLPs) consisting of fully connected (FC) layers:  $A_{tj} = \text{FC}(\mathbf{X}_t, \mathbf{Z}_t; \theta_j)$ , for all  $j = 1, \dots, k$  and for all  $t = 1, \dots, T$ , where  $\theta_j$  are the parameters in the FC layers used to obtain  $A_{tj}$ . We use a single FC hidden layer before the output layer. For binary treatments, the sigmoid activation is used in the output layer. For continuous treatments, MC dropout (Gal & Ghahramani, 2016a) can instead be applied in the FC layers to obtain  $p(A_{tj} \mid \mathbf{X}_j, \mathbf{Z}_j)$ .

To model the probabilistic nature of factor models we incor-

porate variational dropout (Gal & Ghahramani, 2016b) in the RNN as illustrated in Figure 2. Using dropout enables us to obtain samples from  $\mathbf{Z}_t$  and treatment assignments  $A_{t,j}$ . These samples allow us to obtain treatment replicas and to compute predictive checks over time, but also to estimate uncertainty in  $\mathbf{Z}_t$  and potential outcomes.

Using the treatment assignments from the observational dataset, the factor model can be trained using gradient descent based methods. The proposed factor model architecture follows from the theory developed in Section 4 where at each timestep the latent variable  $\mathbf{Z}_t$  is built as a function of the history (parametrised by an RNN). The multitask output is essential for modelling the conditional independence between the assigned treatments given the latent confounder generated by the RNN and the observed covariates. The theory also holds for irregularly sampled data and the proposed factor model can be extended to allow for irregular sampling by using a PhasedLSTM (Neil et al., 2016).

Note that our theory does not put restrictions on the factor model that can be used. Alternative factor models over time are generalized dynamic-factor model (Forni et al., 2000; 2005) or factor-augmented vector autoregressive models (Bernanke et al., 2005). These come from the econometrics literature and explicitly model the dynamics in the data. The use of RNNs in the factor model enables us to learn complex relationships between  $\bar{\mathbf{X}}_t$ ,  $\bar{\mathbf{Z}}_t$  and  $\bar{\mathbf{A}}_t$  from the data, which is needed in medical application involving complex diseases. Nevertheless, predictive checks must always be used to assess any selected factor model.

## 6. Experiments on Synthetic Data

To validate the theory developed in this paper, we perform experiments on synthetic data where we vary the effect of hidden confounding. It is not possible to validate the method on real datasets since the extent of hidden confounding is never known (Wang & Blei, 2019a; Louizos et al., 2017).

### 6.1. Simulated Dataset

To keep the simulation process general, we propose building a dataset using  $p$ -order autoregressive processes. At each timestep  $t$ , we simulate  $k$  time-varying covariates  $X_{t,k}$  representing single cause confounders and a multi-cause hidden confounder  $Z_t$  as follows:

$$X_{t,j} = \frac{1}{p} \sum_{i=1}^p (\alpha_{i,j} X_{t-i,j} + \omega_{i,j} A_{t-i,j}) + \eta_t \quad (8)$$

$$Z_t = \frac{1}{p} \sum_{i=1}^p (\beta_i Z_{t-i} + \sum_{j=1}^k \lambda_{i,j} A_{t-i,j}) + \epsilon_t, \quad (9)$$

for  $j = 1, \dots, k$ ,  $\alpha_{i,k}, \lambda_{i,j} \sim \mathcal{N}(0, 0.5^2)$ ,  $\omega_{i,k}, \beta_i \sim \mathcal{N}(1 - (i/p), (1/p)^2)$ , and  $\eta_t, \epsilon_t \sim \mathcal{N}(0, 0.01^2)$ . The value

of  $Z_t$  changes over time and is affected by the treatment assignment. The treatment assignment  $A_{t,j}$  depend on the single-cause confounder  $X_{t,j}$  and multi-cause hidden confounder  $Z_t$ :

$$\pi_{tj} = \gamma_A \hat{Z}_t + (1 - \gamma_A) \hat{X}_{tj} \quad (10)$$

$$A_{tj} | \pi_{tj} \sim \text{Bernoulli}(\sigma(\lambda \pi_{tj})), \quad (11)$$

where  $\hat{X}_{tj}$  and  $\hat{Z}_t$  are the sum of the covariates and confounders respectively over the last  $p$  timesteps,  $\lambda = 15$ ,  $\sigma(\cdot)$  is the sigmoid and  $\gamma_A$  controls the amount of hidden confounding applied to treatment assignments. The outcome is also obtained as a function of the covariates and hidden confounder:

$$\mathbf{Y}_{t+1} = \gamma_Y Z_{t+1} + (1 - \gamma_Y) \left( \frac{1}{k} \sum_{j=1}^k X_{t+1,j} \right), \quad (12)$$

where  $\gamma_Y$  controls the amount of hidden confounding applied to the outcome. Note that in this case, we repeat the outcome problem, as formulated in Section 3 for each timestep in the sequence.

We simulate datasets consisting of 5000 patients, with trajectories between 20 and 30 timesteps, and  $k = 3$  covariates and treatments. To induce time dependencies we set  $p = 5$ . Each dataset undergoes a 80/10/10 split for training, validation and testing respectively. Hyperparameter optimisation is performed for each trained factor model as explained in the Appendix B.

### 6.2. Evaluating Factor Model using Predictive Checks

Our theory for using the substitute confounders to obtain unbiased treatment responses relies on the fact that the factor model captures well the distribution of the assigned causes.

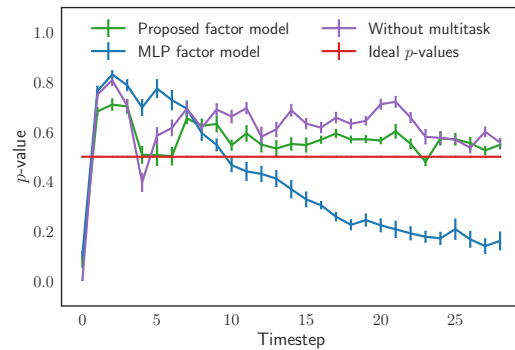


Figure 3. Predictive checks over time. We show the mean  $p$ -values at each timestep and the std error.

To assess the suitability of our proposed factor model architecture, we compare it with the following baselines: RNN

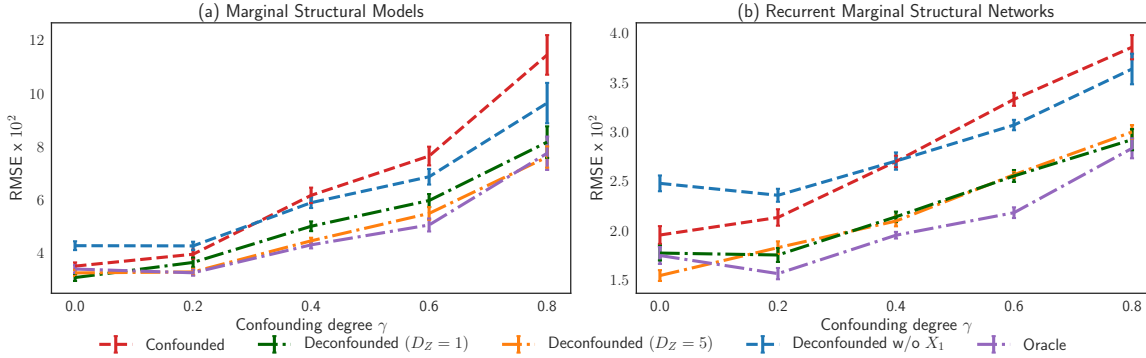


Figure 4. Results for deconfounding one-step ahead predictions of treatment responses in two outcome models: (a) Marginal Structural Models (MSM) and (b) Recurrent Marginal Structural Networks (R-MSN). The average RMSE and the standard error in the results are computed for 30 dataset simulations for each different degree of confounding, as measured by  $\gamma$ .

without multitask output (predicting the  $k$  treatment assignments by passing  $\mathbf{X}_t$  and  $\mathbf{Z}_t$  through a FC layer and output layer with  $k$  neurons) and multilayer perceptron (MLP) used instead of the RNN at each timestep to generate  $\mathbf{Z}_t$ . The MLP factor model does not use the entire history for generating  $\mathbf{Z}_t$ . See Appendix C for details.

Figure 3 shows the  $p$ -values over time computed for the test set in 30 simulated datasets with  $\gamma_A = \gamma_Y = 0.5$ . The  $p$ -values for the MLP factor model decrease over time, which means that there is a consistent distribution mismatch between the treatment assignments learnt by this model and the ones in the test set. Conversely, the predictive checks for our proposed factor model are closer to the ideal  $p$ -value of 0.5. This illustrates that having an architecture capable of capturing time-dependencies and accumulating past information for inferring the latent confounders is crucial. Moreover, the performance for the RNN without multitask is similar to our model, which indicates that the factor model constraint does not affect the performance in capturing the distribution of the causes.

### 6.3. Deconfounding the Estimation of Treatment Responses over Time

We evaluate how well the Time Series Deconfounder can remove hidden confounding bias when used in conjunction with the following outcome models:

**Standard Marginal Structural Models (MSMs).** MSMs (Robins et al., 2000a; Hernán et al., 2001) have been widely used in epidemiology to estimate treatment effects over time. MSMs compute propensity weights using logistic regression to construct a pseudo-population from the observational data that resembles a clinical trial. For full implementation details in Appendix D.1. **Recurrent Marginal Structural Networks (R-MSNs).** R-MSNs (Lim et al., 2018) also apply propensity weighting to adjust for time-dependent confounders, but they estimate the propensity scores using

RNNs instead. The use of RNNs is more robust to changes in the treatment assignment policy. For implementation details, see Appendix D.2.

In the simulated dataset, parameters  $\gamma_A$  and  $\gamma_Y$  control the amount of hidden confounding applied to the treatments and outcomes respectively. We vary this amount through  $\gamma_A = \gamma_Y = \gamma$ . The outcome models are trained without information about  $\bar{\mathbf{Z}}$  (confounded), with the simulated  $\bar{\mathbf{Z}}$  (oracle), as well as after applying the Time Series Deconfounder with different model specifications. To highlight the importance of Assumption 3, we also apply the Time Series Deconfounder after removing the single-cause confounder  $X_1$ , thus violating the assumption.

Figure 4 illustrates the root mean squared error (RMSE) obtained for one-step ahead estimation of treatment responses. The results indicate that the Time Series Deconfounder gives unbiased estimates of treatment responses, i.e. close to the estimates obtained using the simulated (oracle) confounders. The method is robust to model misspecification, performing similarly when  $D_Z = 1$  (simulated size of hidden confounders) and when  $D_Z = 5$  (misspecified size of inferred confounders). When there are no hidden confounders ( $\gamma = 0$ ), the additional information from  $\bar{\mathbf{Z}}$  does not harm the estimations (although they will have higher variance). When Assumption 3 is invalidated, i.e. when  $\bar{\mathbf{Z}}$  are inferred after removing the single cause confounder  $X_1$  from the dataset, we obtain biased estimates. For additional results on a simulated setting with static hidden confounders, see Appendix E.

When the sequential single strong ignorability assumption is invalidated, namely when the latent variables  $\bar{\mathbf{Z}}$  are inferred after removing the single cause confounder  $X_1$  from the dataset, we obtain biased estimates of the treatment responses. The performance in this case, however, is comparable to the performance when there is no control for the hidden confounders.

Table 1. Average RMSE  $\times 10^2$  and the standard error in the results for predicting the effect of antibiotics, vassopressors and mechanical ventilator on three patient covariates. The results are for 10 runs.

Outcome model	White blood cell count		Blood pressure		Oxygen saturation	
	MSM	R-MSN	MSM	R-MSN	MSM	R-MSN
Confounded	$3.90 \pm 0.00$	$2.91 \pm 0.05$	$12.04 \pm 0.00$	$10.29 \pm 0.05$	$2.92 \pm 0.00$	$1.74 \pm 0.03$
Deconfounded ( $D_Z = 1$ )	$3.55 \pm 0.05$	$2.62 \pm 0.07$	$11.69 \pm 0.14$	$9.35 \pm 0.11$	$2.42 \pm 0.02$	$1.24 \pm 0.05$
Deconfounded ( $D_Z = 5$ )	$3.56 \pm 0.04$	$2.41 \pm 0.04$	$11.63 \pm 0.10$	$9.45 \pm 0.10$	$2.43 \pm 0.02$	$1.21 \pm 0.07$
Deconfounded ( $D_Z = 10$ )	$3.58 \pm 0.03$	$2.48 \pm 0.06$	$11.66 \pm 0.14$	$9.20 \pm 0.12$	$2.42 \pm 0.01$	$1.17 \pm 0.06$
Deconfounded ( $D_Z = 20$ )	$3.54 \pm 0.04$	$2.55 \pm 0.05$	$11.57 \pm 0.12$	$9.63 \pm 0.14$	$2.40 \pm 0.01$	$1.28 \pm 0.08$

**Source of gain:** To understand the source of gain in the Time Series Deconfounder, consider why the outcome models fail in the scenarios when there are hidden confounders. MSMs and R-MSNs make the implicit assumption that the treatment assignments depend only on the observed history. The existence of any multi-cause confounders not captured by the history results in biased estimates of both the propensity weights and of the outcomes. On the other hand, the construction in our factor model rules out the existence of any multi-cause confounders which are not captured by  $Z_t$ . By augmenting the data available to the outcome models with the substitute confounders, we eliminate these biases.

## 7. Experiments on MIMIC III

Using the Medical Information Mart for Intensive Care (MIMIC III) (Johnson et al., 2016) database consisting of electronic health records from patients in the ICU, we show how the Time Series Deconfounder can be applied on a real dataset. From MIMIC III we extracted a dataset with 6256 patients for which there are three treatment options at each timestep: antibiotics, vassopressors and mechanical ventilator (all of which can be applied simultaneously). These treatments are common in the ICU and are often used to treat patients with sepsis (Schmidt et al., 2016; Scheeren et al., 2019; Oberst & Sontag, 2019). For each patient, we extracted 25 patient covariates consisting of lab tests and vital signs measured over time that affect the assignment of treatments. We used daily aggregates of the patient covariates and treatments and patient trajectories of up to 50 timesteps. We estimate the effects of antibiotics, vassopressors and mechanical ventilator on the following patient covariates: white blood cell count, blood pressure and oxygen saturation.

Hidden confounding is present in the dataset as patient comorbidities and several lab tests were not included. However, since this is a real dataset, it is not possible to evaluate the extent of hidden confounding or to estimate the true (oracle) treatment responses.

Table 1 illustrates the RMSE when estimating treatment responses by using the MSM and R-MSN outcome models directly on the extracted dataset (Confounded) and after

applying the Time Series Deconfounder and augmenting the dataset with the substitutes for the hidden confounders of different dimensionality  $D_Z$  (Deconfounded). We notice that in all cases, the Time Series Deconfounder enables us to obtain a lower error when estimating the effect of antibiotics, vassopressors and mechanical ventilator on the patients’ white blood cell count, blood pressure and oxygen saturation. By modelling the dependencies in the assigned treatments for each patient, the factor model part of the Time Series Deconfounder was able to infer latent variables that account for the unobserved information about the patient states. Using these substitutes for the hidden confounders in the outcome models resulted in better estimates of the treatment responses. While these results on real data require further validation from doctors (which is outside the scope of this paper), they indicate the potential of the method to be applied in real medical scenarios. See Appendix F for a further discussion and directions for future work.

## 8. Conclusion

The availability of observational data consisting of longitudinal information about patients prompted the development of methods for modelling the effects of treatments on the disease progression in patients. All existing methods make the untestable assumption that there are no hidden confounders. In the longitudinal setting, this assumption is even more problematical than in the static setting. As the state of the patient changes over time and the complexity of the treatment assignments and responses increases, it becomes much easier to miss important confounding information.

We developed the Time Series Deconfounder, a method that takes advantage of the patterns in the multiple treatment assignments over time to infer latent variables that can be used as substitutes for the hidden confounders. Moreover, we developed a deep learning architecture based on an RNN with multitask output and variational dropout for building a factor model over time and computing the substitute confounders in practice. Through experimental results on both synthetic and real datasets, we show the effectiveness of the Time Series Deconfounder in removing the bias from the estimation of treatment responses over time in the presence of multi-cause hidden confounders.



## Acknowledgements

The research presented in this paper was supported by The Alan Turing Institute and the US Office of Naval Research (ONR).

## References

- Abadi, M., Agarwal, A., Barham, P., Brevdo, E., Chen, Z., Citro, C., Corrado, G. S., Davis, A., Dean, J., Devin, M., Ghemawat, S., Goodfellow, I., Harp, A., Irving, G., Isard, M., Jia, Y., Jozefowicz, R., Kaiser, L., Kudlur, M., Levenberg, J., Mané, D., Monga, R., Moore, S., Murray, D., Olah, C., Schuster, M., Shlens, J., Steiner, B., Sutskever, I., Talwar, K., Tucker, P., Vanhoucke, V., Vasudevan, V., Viégas, F., Vinyals, O., Warden, P., Wattenberg, M., Wicke, M., Yu, Y., and Zheng, X. TensorFlow: Large-scale machine learning on heterogeneous systems, 2015. URL <https://www.tensorflow.org/>. Software available from tensorflow.org.
- Alaa, A. and Schaar, M. Limits of estimating heterogeneous treatment effects: Guidelines for practical algorithm design. In *International Conference on Machine Learning*, pp. 129–138, 2018.
- Alaa, A. M. and van der Schaar, M. Bayesian inference of individualized treatment effects using multi-task gaussian processes. In *Advances in Neural Information Processing Systems*, pp. 3424–3432, 2017.
- Bartsch, H., Dally, H., Popanda, O., Risch, A., and Schmezer, P. Genetic risk profiles for cancer susceptibility and therapy response. In *Cancer Prevention*, pp. 19–36. Springer, 2007.
- Bernanke, B. S., Boivin, J., and Elias, P. Measuring the effects of monetary policy: a factor-augmented vector autoregressive (favar) approach. *The Quarterly journal of economics*, 120(1):387–422, 2005.
- Bica, I., Alaa, A. M., Jordon, J., and van der Schaar, M. Estimating counterfactual treatment outcomes over time through adversarially balanced representations. *International Conference on Learning Representations*, 2020.
- DAMour, A. On multi-cause approaches to causal inference with unobserved confounding: Two cautionary failure cases and a promising alternative. In *The 22nd International Conference on Artificial Intelligence and Statistics*, pp. 3478–3486, 2019.
- Forni, M., Hallin, M., Lippi, M., and Reichlin, L. The generalized dynamic-factor model: Identification and estimation. *Review of Economics and statistics*, 82(4):540–554, 2000.
- Forni, M., Hallin, M., Lippi, M., and Reichlin, L. The generalized dynamic factor model: one-sided estimation and forecasting. *Journal of the American Statistical Association*, 100(471):830–840, 2005.
- Gal, Y. and Ghahramani, Z. Dropout as a bayesian approximation: Representing model uncertainty in deep learning. In *international conference on machine learning*, pp. 1050–1059, 2016a.
- Gal, Y. and Ghahramani, Z. A theoretically grounded application of dropout in recurrent neural networks. In *Advances in neural information processing systems*, pp. 1019–1027, 2016b.
- Geng, C., Paganetti, H., and Grassberger, C. Prediction of treatment response for combined chemo-and radiation therapy for non-small cell lung cancer patients using a bio-mathematical model. *Scientific reports*, 7(1):13542, 2017.
- Heckerman, D. Accounting for hidden common causes when inferring cause and effect from observational data. *arXiv preprint arXiv:1801.00727*, 2018.
- Hernán, M. A., Brumback, B., and Robins, J. M. Marginal structural models to estimate the joint causal effect of nonrandomized treatments. *Journal of the American Statistical Association*, 96(454):440–448, 2001.
- Hill, J. L. Bayesian nonparametric modeling for causal inference. *Journal of Computational and Graphical Statistics*, 20(1):217–240, 2011.
- Hochreiter, S. and Schmidhuber, J. Long short-term memory. *Neural computation*, 9(8):1735–1780, 1997.
- Howe, C. J., Cole, S. R., Mehta, S. H., and Kirk, G. D. Estimating the effects of multiple time-varying exposures using joint marginal structural models: alcohol consumption, injection drug use, and hiv acquisition. *Epidemiology (Cambridge, Mass.)*, 23(4):574, 2012.
- Imai, K. and Van Dyk, D. A. Causal inference with general treatment regimes: Generalizing the propensity score. *Journal of the American Statistical Association*, 99(467): 854–866, 2004.
- Johnson, A. E., Pollard, T. J., Shen, L., Li-wei, H. L., Feng, M., Ghassemi, M., Moody, B., Szolovits, P., Celi, L. A., and Mark, R. G. Mimic-iii, a freely accessible critical care database. *Scientific data*, 3:160035, 2016.
- Kallenberg, O. *Foundations of modern probability*. Springer Science & Business Media, 2006.
- Kingma, D. P. and Ba, J. Adam: A method for stochastic optimization. *arXiv preprint arXiv:1412.6980*, 2014.

- Kong, D., Yang, S., and Wang, L. Multi-cause causal inference with unmeasured confounding and binary outcome. *arXiv preprint arXiv:1907.13323*, 2019.
- Kroschinsky, F., Stölzel, F., von Bonin, S., Beutel, G., Kochanek, M., Kiehl, M., and Schellongowski, P. New drugs, new toxicities: severe side effects of modern targeted and immunotherapy of cancer and their management. *Critical Care*, 21(1):89, 2017.
- Lash, T. L., Fox, M. P., MacLehose, R. F., Maldonado, G., McCandless, L. C., and Greenland, S. Good practices for quantitative bias analysis. *International journal of epidemiology*, 43(6):1969–1985, 2014.
- Lee, C., Mastrorarde, N., and van der Schaar, M. Estimation of individual treatment effect in latent confounder models via adversarial learning. *arXiv preprint arXiv:1811.08943*, 2018.
- Lim, B., Alaa, A., and van der Schaar, M. Forecasting treatment responses over time using recurrent marginal structural networks. In *Advances in Neural Information Processing Systems*, pp. 7493–7503, 2018.
- Lok, J. J. et al. Statistical modeling of causal effects in continuous time. *The Annals of Statistics*, 36(3):1464–1507, 2008.
- Louizos, C., Shalit, U., Mooij, J. M., Sontag, D., Zemel, R., and Welling, M. Causal effect inference with deep latent-variable models. In *Advances in Neural Information Processing Systems*, pp. 6446–6456, 2017.
- Miao, W., Geng, Z., and Tchetgen Tchetgen, E. J. Identifying causal effects with proxy variables of an unmeasured confounder. *Biometrika*, 105(4):987–993, 2018.
- Neil, D., Pfeiffer, M., and Liu, S.-C. Phased lstm: Accelerating recurrent network training for long or event-based sequences. In *Advances in neural information processing systems*, pp. 3882–3890, 2016.
- Neyman, J. Sur les applications de la théorie des probabilités aux expériences agricoles: Essai des principes. *Roczniki Nauk Rolniczych*, 10:1–51, 1923.
- Oberst, M. and Sontag, D. Counterfactual off-policy evaluation with gumbel-max structural causal models. *arXiv preprint arXiv:1905.05824*, 2019.
- Pearl, J. *Causality*. Cambridge university press, 2009.
- Platt, R. W., Schisterman, E. F., and Cole, S. R. Time-modified confounding. *American journal of epidemiology*, 170(6):687–694, 2009.
- Ranganath, R. and Perotte, A. Multiple causal inference with latent confounding. *arXiv preprint arXiv:1805.08273*, 2018.
- Ranganath, R., Tang, L., Charlin, L., and Blei, D. Deep exponential families. In *Artificial Intelligence and Statistics*, pp. 762–771, 2015.
- Robins, J. A new approach to causal inference in mortality studies with a sustained exposure period application to control of the healthy worker survivor effect. *Mathematical modelling*, 7(9-12):1393–1512, 1986.
- Robins, J. M. Correcting for non-compliance in randomized trials using structural nested mean models. *Communications in Statistics-Theory and methods*, 23(8):2379–2412, 1994.
- Robins, J. M. and Hernán, M. A. Estimation of the causal effects of time-varying exposures. In *Longitudinal data analysis*, pp. 547–593. Chapman and Hall/CRC, 2008.
- Robins, J. M., Hernan, M. A., and Brumback, B. Marginal structural models and causal inference in epidemiology, 2000a.
- Robins, J. M., Rotnitzky, A., and Scharfstein, D. O. Sensitivity analysis for selection bias and unmeasured confounding in missing data and causal inference models. In *Statistical models in epidemiology, the environment, and clinical trials*, pp. 1–94. Springer, 2000b.
- Roy, J., Lum, K. J., and Daniels, M. J. A bayesian non-parametric approach to marginal structural models for point treatments and a continuous or survival outcome. *Biostatistics*, 18(1):32–47, 2016.
- Rubin, D. B. Bayesian inference for causal effects: The role of randomization. *The Annals of statistics*, pp. 34–58, 1978.
- Rubin, D. B. Bayesianly justifiable and relevant frequency calculations for the applies statistician. *The Annals of Statistics*, pp. 1151–1172, 1984.
- Scharfstein, D., McDermott, A., Díaz, I., Carone, M., Lunardon, N., and Turkoz, I. Global sensitivity analysis for repeated measures studies with informative drop-out: A semi-parametric approach. *Biometrics*, 74(1):207–219, 2018.
- Scheeren, T. W., Bakker, J., De Backer, D., Annane, D., Asfar, P., Boerma, E. C., Cecconi, M., Dubin, A., Dünser, M. W., Duranteau, J., et al. Current use of vasopressors in septic shock. *Annals of intensive care*, 9(1):20, 2019.
- Schmidt, G. A., Mandel, J., Sexton, D. J., and Hockberger, R. S. Evaluation and management of suspected sepsis

and septic shock in adults. *UpToDate*. Available online: <https://www.uptodate.com/contents/evaluation-and-management-of-suspected-sepsisand-septic-shock-in-adults> (accessed on 29 September 2017), 2016.

Schulam, P. and Saria, S. Reliable decision support using counterfactual models. In *Advances in Neural Information Processing Systems*, pp. 1697–1708, 2017.

Soleimani, H., Subbaswamy, A., and Saria, S. Treatment-response models for counterfactual reasoning with continuous-time, continuous-valued interventions. *arXiv preprint arXiv:1704.02038*, 2017.

Tipping, M. E. and Bishop, C. M. Probabilistic principal component analysis. *Journal of the Royal Statistical Society: Series B (Statistical Methodology)*, 61(3):611–622, 1999.

Tran, D. and Blei, D. M. Implicit causal models for genome-wide association studies. *arXiv preprint arXiv:1710.10742*, 2017.

Vlachostergios, P. J. and Faltas, B. M. Treatment resistance in urothelial carcinoma: an evolutionary perspective. *Nature Reviews Clinical Oncology*, pp. 1, 2018.

Wager, S. and Athey, S. Estimation and inference of heterogeneous treatment effects using random forests. *Journal of the American Statistical Association*, 2017.

Wang, Y. and Blei, D. M. The blessings of multiple causes. *Journal of the American Statistical Association*, (just-accepted):1–71, 2019a.

Wang, Y. and Blei, D. M. Multiple causes: A causal graphical view. *arXiv preprint arXiv:1905.12793*, 2019b.

Xu, Y., Xu, Y., and Saria, S. A bayesian nonparametric approach for estimating individualized treatment-response curves. In *Machine Learning for Healthcare Conference*, pp. 282–300, 2016.

Yoon, J., Jordon, J., and van der Schaar, M. Ganite: Estimation of individualized treatment effects using generative adversarial nets. *International Conference on Learning Representations (ICLR)*, 2018.

## A. Proof for Theorem 1

Before proving Theorem 1, we introduce several definitions and Lemmas that will aid with the proof. Note that these are extended from the static setting in Wang & Blei (2019a).

Remember that at each timestep  $t$ , the random variable  $\mathbf{Z}_t \in \mathcal{Z}_t$  is constructed as a function of the history until timestep  $t$ :  $\mathbf{Z}_t = g(\bar{\mathbf{H}}_{t-1})$ , where  $\bar{\mathbf{H}}_{t-1} = (\bar{\mathbf{Z}}_{t-1}, \bar{\mathbf{X}}_{t-1}, \bar{\mathbf{A}}_{t-1})$  takes values in  $\bar{\mathcal{H}}_{t-1} = \bar{\mathcal{Z}}_{t-1} \times \bar{\mathcal{X}}_{t-1} \times \bar{\mathcal{A}}_{t-1}$  and  $g: \bar{\mathcal{H}}_{t-1} \rightarrow \mathcal{Z}_t$ .

In order to obtain **sequential ignorable treatment assignment** using the substitutes for the hidden confounders  $\mathbf{Z}_t$ , the following property needs to hold:

$$\mathbf{Y}(\bar{\mathbf{a}}) \perp\!\!\!\perp (A_{t1}, \dots, A_{tk}) \mid \bar{\mathbf{X}}_t, \bar{\mathbf{A}}_{t-1}, \bar{\mathbf{Z}}_t, \quad (13)$$

$\forall \bar{\mathbf{a}} \in \bar{\mathcal{A}}$  and  $\forall t \in \{0, \dots, T\}$ .

### Definition: Sequential Kallenberg construction

At timestep  $t$ , we say that the distribution of assigned causes  $(A_{t1}, \dots, A_{tk})$  admits a sequential Kallenberg construction from random variables  $\mathbf{Z}_t = g(\bar{\mathbf{H}}_{t-1})$  and  $\mathbf{X}_t$  if there exist measurable functions  $f_{tj}: \mathcal{Z}_t \times \mathcal{X}_t \times [0, 1] \rightarrow \mathcal{A}_j$  and random variables  $U_{jt} \in [0, 1]$ , with  $j = 1, \dots, k$  such that:

$$A_{tj} = f_{tj}(\mathbf{Z}_t, \mathbf{X}_t, U_{tj}), \quad (14)$$

where  $U_{tj}$  marginally follow Uniform $[0, 1]$  and jointly satisfy:

$$(U_{t1}, \dots, U_{tk}) \perp\!\!\!\perp \mathbf{Y}(\bar{\mathbf{a}}) \mid \mathbf{Z}_t, \mathbf{X}_t, \bar{\mathbf{H}}_{t-1}, \quad (15)$$

for all  $\bar{\mathbf{a}} \in \bar{\mathcal{A}}$ .

**Lemma 1: Sequential Kallenberg construction at each timestep  $t \Rightarrow$  Sequential strong ignorability.** If at every timestep  $t$ , the distribution of assigned causes  $(A_{t1}, \dots, A_{tk})$  admits a Kallenberg construction from  $\mathbf{Z}_t = g(\bar{\mathbf{H}}_{t-1})$  and  $\mathbf{X}_t$  then we obtain sequential strong ignorability.

**Proof for Lemma 1:** Assume  $\mathcal{A}_j, j = 1, \dots, m$  are Borel spaces.

For any  $t \in \{1, \dots, T\}$  assume  $\mathcal{Z}_t$  and  $\mathcal{X}_t$  are measurable spaces and assume that  $A_{tj} = f_{tj}(\mathbf{Z}_t, \mathbf{X}_t, U_{tj})$ , where  $f_{tj}$  are measurable and

$$(U_{t1}, \dots, U_{tk}) \perp\!\!\!\perp \mathbf{Y}(\bar{\mathbf{a}}) \mid \mathbf{Z}_t, \mathbf{X}_t, \bar{\mathbf{H}}_{t-1}, \quad (16)$$

for all  $\bar{\mathbf{a}} \in \bar{\mathcal{A}}$ . This implies that:

$$(\mathbf{Z}_t, \mathbf{X}_t, U_{t1}, \dots, U_{tk}) \perp\!\!\!\perp \mathbf{Y}(\bar{\mathbf{a}}) \mid \mathbf{Z}_t, \mathbf{X}_t, \bar{\mathbf{H}}_{t-1}. \quad (17)$$

Since the  $A_{tj}$ 's are measurable functions of  $(\mathbf{Z}_t, \mathbf{X}_t, U_{t1}, \dots, U_{tk})$  and  $\bar{\mathbf{H}}_{t-1} = (\bar{\mathbf{Z}}_{t-1}, \bar{\mathbf{X}}_{t-1}, \bar{\mathbf{A}}_{t-1})$ , we have that sequential strong ignorability holds:

$$(A_{t1}, \dots, A_{tk}) \perp\!\!\!\perp \mathbf{Y}(\bar{\mathbf{a}}) \mid \bar{\mathbf{X}}_t, \bar{\mathbf{A}}_{t-1}, \bar{\mathbf{Z}}_t, \quad (18)$$

$\forall \bar{\mathbf{a}} \in \bar{\mathcal{A}}$  and  $\forall t \in \{0, \dots, T\}$ .

**Lemma 2: Factor models for the assigned causes  $\Rightarrow$  Sequential Kallenberg construction at each timestep  $t$ .** Under weak regularity conditions, if the distribution of assigned causes  $p(\bar{\mathbf{a}})$  can be written as the factor model  $p(\theta_{1:k}, \bar{\mathbf{x}}, \bar{\mathbf{z}}, \bar{\mathbf{a}})$  then we obtain a sequential Kallenberg construction for each timestep.

Regularity condition: The domains of the causes  $\mathcal{A}_j$  for  $j = 1, \dots, k$  are Borel subsets of compact intervals. Without loss of generality, assume  $\mathcal{A}_j = [0, 1]$  for  $j = 1, \dots, k$ .

The proof for Lemma 2 uses Lemma 2.22 in (Kallenberg, 2006) (kernels and randomization): Let  $\mu$  be a probability kernel from a measurable space  $S$  to a Borel space  $T$ . Then there exists some measurable function  $f: S \times [0, 1] \rightarrow T$  such that if  $\vartheta$  is  $U(0, 1)$ , then  $f(s, \vartheta)$  has distribution  $\mu(s, \cdot)$  for every  $s \in S$ .

**Proof for Lemma 2:** For timestep  $t$ , consider the random variables  $A_{t1} \in \mathcal{A}_1, \dots, A_{tk} \in \mathcal{A}_k, \mathbf{X}_t \in \mathcal{X}_t, \mathbf{Z}_t = g(\bar{\mathbf{H}}_{t-1}) \in \mathcal{Z}_t$  and  $\theta_j \in \Theta$ . Assume sequential single strong ignorability holds. Without loss of generality, assume  $\mathcal{A}_j = [0, 1]$  for  $j = 1, \dots, k$ .

From Lemma 2.22 in Kallenberg (1997), there exists some measurable function  $f_{tj}: \mathcal{Z}_t \times \mathcal{X}_t \times [0, 1] \rightarrow [0, 1]$  such that  $U_{tj} \sim \text{Uniform}[0, 1]$  and:

$$A_{tj} = f_{tj}(\mathbf{Z}_t, \mathbf{X}_t, U_{tj}) \quad (19)$$

and there exists some measurable function  $h_{tj} : \Theta \times [0, 1] \rightarrow [0, 1]$  such that:

$$U_{tj} = h_{tj}(\theta_j, \omega_{tj}), \quad (20)$$

where  $\omega_{tj} \sim \text{Uniform}[0, 1]$  and  $j = 1, \dots, k$ .

From our definition of the factor model we have that  $\omega_{tj}$  for  $j = 1, \dots, k$  are jointly independent. Otherwise,  $A_{tj} = f_{tj}(\mathbf{Z}_t, \mathbf{X}_t, h_{tj}(\theta_j, \omega_{tj}))$  would not have been conditionally independent given  $\mathbf{Z}_t, \mathbf{X}_t$ .

Since sequential single strong ignorability holds at each timestep  $t$ , we have that  $A_{tj} \perp\!\!\!\perp \mathbf{Y}(\bar{\mathbf{a}}) \mid \mathbf{X}_t, \bar{\mathbf{H}}_{t-1} \forall \bar{\mathbf{a}} \in \bar{\mathcal{A}}, \forall t \in \{0, \dots, T\}$  and for  $j = 1, \dots, k$  which implies:

$$\omega_{tj} \perp\!\!\!\perp \mathbf{Y}(\bar{\mathbf{a}}) \mid \mathbf{X}_t, \bar{\mathbf{H}}_{t-1}, \quad (21)$$

$\forall \bar{\mathbf{a}} \in \bar{\mathcal{A}}$  and  $\forall j \in \{1, \dots, k\}$ .

Using this, we can write:

$$\begin{aligned} p(Y(\bar{\mathbf{a}}), \omega_{t1}, \dots, \omega_{tk} \mid \mathbf{X}_t, \bar{\mathbf{H}}_{t-1}) &= p(Y(\bar{\mathbf{a}}) \mid \mathbf{X}_t, \bar{\mathbf{H}}_{t-1}) \cdot p(\omega_{t1}, \dots, \omega_{tk} \mid Y(\bar{\mathbf{a}}), \mathbf{X}_t, \bar{\mathbf{H}}_{t-1}) \\ &= p(Y(\bar{\mathbf{a}}) \mid \mathbf{X}_t, \bar{\mathbf{H}}_{t-1}) \cdot \prod_{j=1}^k p(\omega_{tj} \mid \omega_{t1}, \dots, \omega_{t,j-1}, Y(\bar{\mathbf{a}}), \mathbf{X}_t, \bar{\mathbf{H}}_{t-1}) \\ &= p(Y(\bar{\mathbf{a}}) \mid \mathbf{X}_t, \bar{\mathbf{H}}_{t-1}) \cdot \prod_{j=1}^k p(\omega_{tj} \mid \mathbf{X}_t, \bar{\mathbf{H}}_{t-1}) \\ &= p(Y(\bar{\mathbf{a}}) \mid \mathbf{X}_t, \bar{\mathbf{H}}_{t-1}) \cdot p(\omega_{t1}, \dots, \omega_{tk} \mid \mathbf{X}_t, \bar{\mathbf{H}}_{t-1}) \end{aligned}$$

where the second and third steps follow from equation (21) and the fact that  $\omega_{t1}, \dots, \omega_{tk}$  are jointly independent. This gives us:

$$(\omega_{t1}, \dots, \omega_{tk}) \perp\!\!\!\perp \mathbf{Y}(\bar{\mathbf{a}}) \mid \mathbf{X}_t, \bar{\mathbf{H}}_{t-1} \quad (22)$$

Moreover, since the latent random variable  $\mathbf{Z}_t$  is constructed without knowledge of  $\mathbf{Y}(\bar{\mathbf{a}})$ , but rather as a function of the history  $\bar{\mathbf{H}}_{t-1}$  we have:

$$(\omega_{t1}, \dots, \omega_{tk}) \perp\!\!\!\perp \mathbf{Y}(\bar{\mathbf{a}}) \mid \mathbf{Z}_t, \mathbf{X}_t, \bar{\mathbf{H}}_{t-1}. \quad (23)$$

$\theta_{1:k}$  are parameters in the factor model and can be considered point masses, so we also have that:

$$(\theta_1, \dots, \theta_k) \perp\!\!\!\perp \mathbf{Y}(\bar{\mathbf{a}}) \mid \mathbf{Z}_t, \mathbf{X}_t, \bar{\mathbf{H}}_{t-1}, \quad (24)$$

Since  $U_{tj} = (h_{ij}(\theta_j, \omega_{tj}))$  are measurable functions of  $\theta_j$  and  $\omega_{tj}$  we have that:

$$(U_{t1}, \dots, U_{tk}) \perp\!\!\!\perp \mathbf{Y}(\bar{\mathbf{a}}) \mid \mathbf{Z}_t, \mathbf{X}_t, \bar{\mathbf{H}}_{t-1} \quad (25)$$

We have thus obtained a sequential Kallenberg construction at timestep  $t$ .

**Theorem 1:** If the distribution of the assigned causes  $p(\bar{\mathbf{a}}_{1:M})$  can be written as the factor model  $p(\theta_{1:k}, \bar{\mathbf{x}}, \bar{\mathbf{z}}, \bar{\mathbf{a}})$  then we obtain *sequential ignorable treatment assignment*:

$$\mathbf{Y}(\bar{\mathbf{a}}) \perp\!\!\!\perp (A_{t1}, \dots, A_{tk}) \mid \bar{\mathbf{X}}_t, \bar{\mathbf{Z}}_t, \bar{\mathbf{A}}_{t-1}, \quad (26)$$

for all  $\bar{\mathbf{a}} \in \bar{\mathcal{A}}$  and for all  $t \in \{0, \dots, T\}$ .

**Proof for Theorem 1:**

Theorem 1 follows from Lemmas 1 and 2. In particular, using the proposed factor graph, we can obtain a sequential Kallenberg construction at each timestep and then obtain sequential ignorability.

## B. Implementation details for the factor model

The factor model described in Section 5 was implemented in Tensorflow (Abadi et al., 2015) and trained on an NVIDIA Tesla K80 GPU. For each synthetic dataset (simulated as described in Section 6.1), we obtained 5000 patients, out of which 4000 were used for training, 500 for validation and 500 for testing. Using the validation set, we perform hyperparameter optimisation using 30 iterations of random search to find the optimal values for the learning rate, minibatch size (M), RNN hidden units, multitask FC hidden units and RNN dropout probability. LSTM (Hochreiter & Schmidhuber, 1997) units are used for the RNN implementation. The search range for each hyperparameter is described in Table 2.

The trajectories for the patients do not necessarily have to be equal. However, to be able to train the factor model, we zero padded them such that they all had the same length. The patient trajectories were then grouped into minibatches of size M and the factor model was trained using the Adam optimiser (Kingma & Ba, 2014) for 100 epochs.

Table 2. Hyperparameter search range for the proposed factor model implemented using a recurrent neural network with multitask output and variational dropout.

Hyperparameter	Search range
Learning rate	0.01, 0.001, 0.0001
Minibatch size	64, 128, 256
RNN hidden units	32, 64, 128, 256
Multitask FC hidden units	32, 64, 128
RNN dropout probability	0.1, 0.2, 0.3, 0.4, 0.5

Table 3 illustrates the optimal hyperparameters obtained for the factor model under the different amounts of hidden confounding applied (as described by the experiments in Section 6.1). Since the results for assessing the Time Series Deconfounder are averaged across 30 different simulated datasets, we report here the optimal hyperparameters identified through majority voting. We note that when the effect of the hidden confounders on the treatment assignments and the outcome is large, more capacity is needed in the factor model to be able to infer them.

Table 3. Optimal hyperparameters for the factor model when different amounts of hidden confounding are applied in the synthetic dataset. The parameter  $\gamma$  measures the amount of hidden confounding applied.

Hyperparameter	$\gamma = 0$	$\gamma = 0.2$	$\gamma = 0.4$	$\gamma = 0.6$	$\gamma = 0.8$
Learning rate	0.01	0.01	0.01	0.01	0.001
Minibatch size	64	64	64	64	128
RNN hidden units	32	64	64	128	128
Multitask FC hidden units	64	128	64	128	128
RNN dropout probability	0.2	0.2	0.1	0.3	0.3

## C. Baselines for evaluating factor model

Figure 5 illustrates the architecture at each timestep for our proposed factor model and for the baselines used for comparison. Figure 5(a) represents our proposed architecture for the factor model consisting of a recurrent neural network with multitask output and variational dropout. We want to ensure that the multitask constraint does not cause a decrease in the capability of the network to capture the distribution of the assigned causes. In order to do so, we compare our proposed factor model with the network in Figure 5(b) where we predict the  $k$  treatment assignments by passing  $\mathbf{X}_t$  and  $\mathbf{Z}_t$  through a hidden layer and having an output layer with  $k$  neurons. Moreover, to highlight the importance of learning time-dependencies in order to estimate the substitutes for the hidden confounders, we also use as a baseline the factor model in Figure 5(c). In this case, a multilayer perceptron (MLP) is shared across the timesteps and it infers the latent variable  $Z_t$  using only the previous covariates and treatments. Note that in this case there is no dependency on the entire history.

The baselines were optimised under the same set-up described for our proposed factor model in Appendix B. Tables 4 and 5 describe the search ranges used for the hyperparameters in each of the baselines.

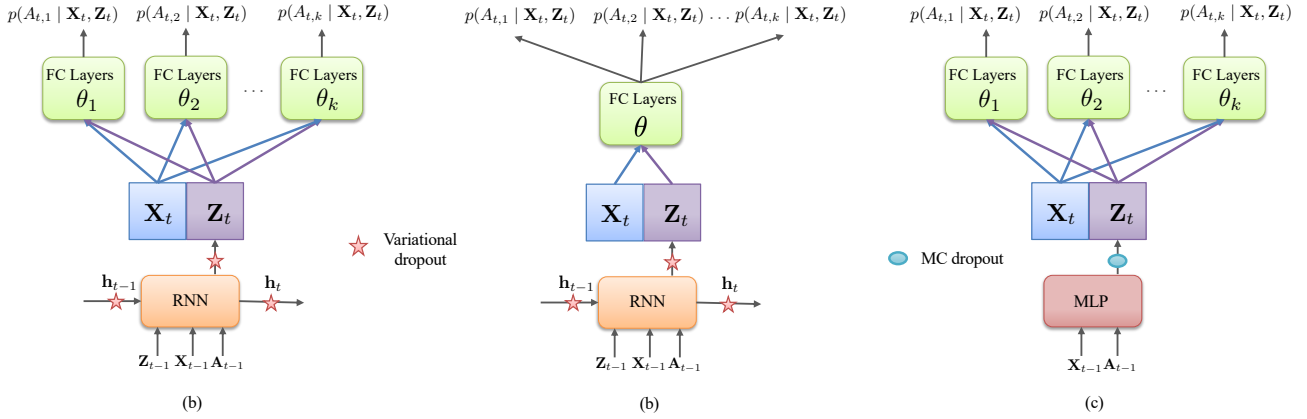


Figure 5. (a) Proposed factor model using recurrent neural network with multitask output and variational dropout. (b) Alternative design without multitask output. (c) Factor model using an MLP (shared across timestep) and multitask output. This baseline does not capture time-dependencies. MC dropout (Gal & Ghahramani, 2016a) is applied in the MLP to be able to sample from the substitute hidden confounders.

Table 4. Hyperparameter search range for factor model without multitask (Figure 5(b)).

Hyperparameter	Search range
Learning rate	0.01, 0.001, 0.0001
Minibatch size	64, 128, 256
Max gradient norm	1.0, 2.0, 4.0
RNN hidden units	32, 64, 128, 256
Multitask FC hidden units	32, 64, 128
RNN dropout probability	0.1, 0.2, 0.3, 0.4, 0.5

## D. Outcome models

After inferring the substitutes for the hidden confounders using the factor model, we implement outcome models to estimate the individualised treatment responses:

$$\mathbb{E}[Y_{t+1} | \bar{\mathbf{A}}_t, \bar{\mathbf{X}}_t, \bar{\mathbf{Z}}_t] = h(\bar{\mathbf{A}}_t, \bar{\mathbf{X}}_t, \bar{\mathbf{Z}}_t) \quad (27)$$

Note that, by setting  $t = T$  this is equivalent to the problem formulation in Section 3. However, in this case, we repeat the outcome problem, as formulated in Section 3 for each timestep in the sequence. Thus, we train the outcome models and evaluate them on predicting the treatment responses for each timestep, i.e. one-step-ahead predictions.

For training and tuning the outcome models, we use the same train/validation/test splits that we have used for the factor model. This means that the substitutes for the hidden confounders estimated using the fitted factor model on the test set are also used for testing purposes in the outcome models.

### D.1. Marginal Structural Models

MSMs (Robins et al., 2000a; Hernán et al., 2001) have been widely used in epidemiology to perform causal inference in longitudinal data. MSMs compute propensity weights to construct a pseudo-population from the observational data that resembles the one in a clinical trial and thus remove the selection bias and the bias introduced by time-dependent confounders (Platt et al., 2009). The propensity scores for each patient in the training set are computed as follows:

$$SW = \prod_{i=1}^t \frac{f(\mathbf{A}_t | \bar{\mathbf{A}}_{t-1})}{f(\mathbf{A}_t | \bar{\mathbf{X}}_t, \bar{\mathbf{Z}}_t, \bar{\mathbf{A}}_{t-1})} = \prod_{i=1}^t \frac{\prod_{j=1}^k f(A_{t,j} | \bar{\mathbf{A}}_{t-1})}{\prod_{j=1}^k f(A_{t,j} | \bar{\mathbf{X}}_t, \bar{\mathbf{Z}}_t, \bar{\mathbf{A}}_{t-1})} \quad (28)$$

Table 5. Hyperparameter search range for MLP factor model. Figure 5(c))

Hyperparameter	Search range
Learning rate	0.01, 0.001, 0.0001
Minibatch size	64, 128, 256
MLP hidden layer size	32, 64, 128, 256
Multitask FC hidden units	32, 64, 128
MLP dropout probability	0.1, 0.2, 0.3, 0.4, 0.5

where  $f(\cdot)$  is the conditional probability mass function for discrete treatments and the conditional probability density function for continuous treatments.

We adopt the implementation in [Hernán et al. \(2001\)](#); [Howe et al. \(2012\)](#) for MSMs and estimate the propensity weights using logistic regression as follows:

$$f(A_{t,k} | \bar{\mathbf{A}}_{t-1}) = \sigma \left( \sum_{j=1}^k \omega_k \left( \sum_{i=1}^{t-1} A_{t,j} \right) \right) \quad (29)$$

$$f(A_{t,k} | \bar{\mathbf{X}}_t, \bar{\mathbf{Z}}_t, \bar{\mathbf{A}}_{t-1}) = \sigma \left( \sum_{j=1}^k \phi_k \left( \sum_{i=1}^{t-1} A_{t,j} \right) + \mathbf{w}_1 \mathbf{X}_t + \mathbf{w}_2 \mathbf{X}_{t-1} + \mathbf{w}_3 \mathbf{Z}_t + \mathbf{w}_4 \mathbf{Z}_{t-1} \right) \quad (30)$$

where  $\omega_*$ ,  $\phi_*$  and  $\mathbf{w}_*$  are regression coefficients and  $\sigma(\cdot)$  is the sigmoid function.

For predicting the outcome, the following regression model is used, where each individual patient is weighted by its propensity score:

$$h(\bar{\mathbf{A}}_t, \bar{\mathbf{X}}_t, \bar{\mathbf{Z}}_t) = \sum_{j=1}^k \beta_k \left( \sum_{i=1}^t A_{t,j} \right) + \mathbf{l}_1 \mathbf{X}_t + \mathbf{l}_2 \mathbf{X}_{t-1} + \mathbf{l}_3 \mathbf{Z}_t + \mathbf{l}_4 \mathbf{Z}_{t-1} \quad (31)$$

where  $\beta_*$  and  $\mathbf{l}_*$  are regression coefficients. Since MSMs do not require hyperparameter tuning, we train them on the patients from both the train and validation sets.

## D.2. Recurrent Marginal Structural Networks

R-MSNs, implemented as described in [Lim et al. \(2018\)](#)<sup>3</sup>, use recurrent neural networks to estimate the propensity scores and to build the outcome model. The use of RNNs is more robust to changes in the treatment assignment policy. Moreover, R-MSNs represent the first application of deep learning in predicting time-dependent effects. The propensity weights are estimated using recurrent neural networks as follows:

$$f(A_{t,k} | \bar{\mathbf{A}}_{t-1}) = \text{RNN}_1(\bar{\mathbf{A}}_{t-1}) \quad f(A_{t,k} | \bar{\mathbf{X}}_t, \bar{\mathbf{Z}}_t, \bar{\mathbf{A}}_{t-1}) = \text{RNN}_2(\bar{\mathbf{X}}_t, \bar{\mathbf{Z}}_t, \bar{\mathbf{A}}_{t-1}) \quad (32)$$

For predicting the outcome, the following prediction network is used:

$$h(\bar{\mathbf{A}}_t, \bar{\mathbf{X}}_t, \bar{\mathbf{Z}}_t) = \text{RNN}_3(\bar{\mathbf{X}}_t, \bar{\mathbf{Z}}_t, \bar{\mathbf{A}}_t), \quad (33)$$

where in the loss function, each patient is weighted by its propensity score. Since the purpose of our method is not to improve predictions, but rather to assess how well the R-MSNs can be deconfounded using our method, we use the optimal hyperparameters for this model, as identified by [Lim et al. \(2018\)](#). R-MSNs are then trained on the combined set of patients from the training and validation sets.

R-MSNs ([Lim et al., 2018](#)), can also be used to forecast treatment responses for an arbitrary number of steps in the future. In our paper we focus on one-step ahead predictions of the treatment responses. However, the Time Series Deconfounder can also be applied for the long-term estimation of treatment effects.

<sup>3</sup>We used the publicly available implementation from [https://github.com/sjblim/rmsn\\_nips\\_2018](https://github.com/sjblim/rmsn_nips_2018).



Table 6. Hyperparameters used for R-MSN.

Hyperparameter	Propensity networks		Prediction network
	$f(\mathbf{A}_t   \bar{\mathbf{A}}_{t-1})$	$f(\mathbf{A}_t   \bar{\mathbf{H}}_t)$	
Dropout rate	0.1	0.1	0.1
State size	6	16	16
Minibatch size	128	64	128
Learning rate	0.01	0.01	0.01
Max norm	2.0	1.0	0.5

### E. Model of Tumour Growth

To show the applicability of our method in a more realistic simulation, we use the pharmacokinetic-pharmacodynamic (PK-PD) model of tumour growth under the effects of chemotherapy and radiotherapy proposed by (Geng et al., 2017). The tumour volume after  $t$  days since diagnosis is modelled as follows:

$$V(t) = \left( \underbrace{1 + \rho \log\left(\frac{K}{V(t-1)}\right)}_{\text{Tumor growth}} - \underbrace{\beta_c C(t)}_{\text{Chemotherapy}} - \underbrace{(\alpha_r d(t) + \beta_r d(t)^2)}_{\text{Radiotherapy}} + \underbrace{e_t}_{\text{Noise}} \right) V(t-1) \tag{34}$$

where  $K, \rho, \beta_c, \alpha_r, \beta_r, e_t$  are sampled as described in Geng et al. (2017).  $C(t)$  is the chemotherapy drug concentration and  $d(t)$  is the dose of radiation. Chemotherapy and radiotherapy prescriptions are modelled as Bernoulli random variables that depend on the tumour size. Full details about treatments are in Lim et al. (2018).

Table 7. Average RMSE  $\times 10^2$  (normalised by the maximum tumour volume) and the standard error in the results for predicting the effect of chemotherapy and radiotherapy on the tumour volume.

Outcome model	MSM	R-MSN
Confounded	7.29 $\pm$ 0.14	5.31 $\pm$ 0.16
Deconfounded ( $D_Z = 1$ )	6.47 $\pm$ 0.16	4.76 $\pm$ 0.17
Deconfounded ( $D_Z = 5$ )	6.25 $\pm$ 0.14	4.79 $\pm$ 0.19
Deconfounded ( $D_Z = 10$ )	6.31 $\pm$ 0.11	4.54 $\pm$ 0.17
Oracle	6.92 $\pm$ 0.19	5.00 $\pm$ 0.15

To account for patient heterogeneity due to genetic features (Bartsch et al., 2007), the prior means for  $\beta_c$  and  $\alpha_r$  are adjusted according to three patient subgroups as described in Lim et al. (2018). The patient subgroup  $S^{(i)} \in \{1, 2, 3\}$  represents a confounder because it affects the tumour growth and subsequently the treatment assignments. We reproduced the experimental set-up in Lim et al. (2018) and simulated datasets with 10000 patients for training, 1000 for validation and 1000 for testing. We simulated 30 datasets and averaged the results for testing the MSM and R-MSN outcome models without the information about patient types (confounded), with the true simulated patient types, as well as after applying the Time Series Deconfounder with  $D_Z \in \{1, 5, 10\}$ .

The results in Table 7 indicate that our method can infer substitutes for static hidden confounders such as patient subgroups which affect the treatment responses over time. By construction,  $\bar{\mathbf{Z}}$  also captures time dependencies which helps with the prediction of outcomes. This is why the performance of the deconfounded models is slightly better than of the oracle model which uses static patient groups.

## F. Discussion

The Time Series Deconfounder firstly builds a factor model to infer substitutes for the hidden confounders. If the fitted factor model captures well the distribution of the assigned causes, which can be assessed through predictive checks, the substitutes for the hidden confounders help us obtain sequential strong ignorability (Theorem 1). Then, the Time Series Deconfounder uses the inferred substitutes for the hidden confounders in an outcome model that estimates individualized treatment responses. The experimental results show the applicability of the Time Series Deconfounder both in a controlled simulated settings and in a real dataset consisting of electronic health records from patients in the ICU. In these settings, the Time Series Deconfounder was able to remove the bias from hidden confounders when estimating treatment responses conditional on patient history.

In the static causal inference setting, several methods have been proposed to extend the deconfounder algorithm in (Wang & Blei, 2019a). For instance, (Wang & Blei, 2019b) augment the theory in the deconfounder algorithm in (Wang & Blei, 2019a) by extending it to causal graphs. Moreover, (Wang & Blei, 2019b) show that by using some of the causes as proxies of the shared confounder in the outcome model one can identify the effects of the others causes. DAmour (2019) also suggests using proxy variables to obtain non-parametric identification of the mean potential outcomes (Miao et al., 2018). Additionally, Kong et al. (2019) prove that identification of causal effects is possible in the multi-cause setting when the treatments are normally distributed and the outcome is binary and follows a logistic structural equation model.

For the Time Series Deconfounder, similarly to Wang & Blei (2019a), identifiability can be assessed by computing the uncertainty in the outcome model estimates, as described in Section 4.2. When the treatment effects are non-identifiable, the Time Series Deconfounder estimates will have high variance. Thus, future work could explore building upon the results in (Wang & Blei, 2019b) and (DAmour, 2019) and using proxy variables in the outcome model to prove identifiability of causal estimates in the multi-cause time series setting.